

Ray Theory of Waves

K. F. Ren^{1,2*}, M. Yang^{3*}, Q. Duan², C. Rozé¹, C. Zhang^{1,4} and X. Han^{2*}

¹CORIA/UMR 6614 CNRS - University of Rouen Normandy BP 12, 76801 Saint-Etienne du Rouvray, France

²School of Physics, Xidian University, Xi'an 710071, China

³Institute of Radio Frequency Technology and Software, School of Integrated Circuits and Electronics, Beijing Institute of Technology (BIT), Beijing 100081, China

⁴School of Information Science and Engineering, Southeast University, Nanjing 210096, China*

(Dated: March 22, 2024)

In order to deal with the interaction of an electromagnetic wave with large homogeneous objects of arbitrary shape with smooth surface we develop the *ray theory of waves* (RTW) which is composed of the *vectorial complex ray model* (VCRM) and VCRM based singularity theory. By introducing the wavefront curvature as an intrinsic property of rays, VCRM permits to predict the amplitude and the phase of field at any point rigorously in the sense of ray model. Its combination with the singularity theory remedies the discontinuity in the ray model. In this letter, the wavefront equation, key physical law of VCRM describing the relation between the wavefront curvatures of the incident wave and the refracted/reflected wave, is derived for the most general case of three dimension scattering. The strategy of the calculation scheme in RTW is described. Typical applications to the prediction of the rainbow patterns of a spheroidal drop are presented. The comparison to a rigorous numerical method, multilevel fast multipole algorithm, shows that RTW can predict very fast and precisely the scattered field even in the vicinity of caustics.

Introduction – The interaction of waves (light, electromagnetic or acoustic waves) with large macroscopic objects concern great number of research domains. Though the fundamental laws (Maxwell equations, etc.) have been well established, their applications to practical problems are always challenging. For example, the scientific community has not efficient methods to predict with precision the scattered field of a wave by objects of complex forms and size much larger than the wavelength. This fact has important impact on the scientific research and the engineering design. In fact, researchers have made great efforts to improve this situation. Many sophisticated numerical techniques have been developed in the field of electromagnetic computation [20, 25], such as the multilevel fast multipole algorithm (MLFMA)[26]. These methods can be applied to objects of complex shape and composition but they are resource and time consuming. The calculable size is also limited (less than 200 wavelengths for dielectric objects[24]). Some rigorous solutions exist for the particles of simple shapes (spheroid, ellipsoid), but the calculable size is still at the same order as the pure numerical methods. Different approximate methods have also been investigated to deal with specific problems or in specific conditions[2, 7, 17, 18, 25]. For instance, the catastrophe theory provides a powerful tool to study the morphology of the scattering patterns near caustics and its classification by using polynomial functions[2, 4]. So, we are still lack of efficient methods to simulate directly with precision the scattering patterns of real large objects.

The *Ray Theory of Waves* (RTW) presented in this letter intends to reply this demand. It consists of the Vectorial Complex Ray Model (VCRM)[12, 19] and its combination with singularity theory[6] by using the uniform approximation[5]. Its four *principles* are: (i). All

waves are described by the vectorial complex rays and each ray possesses three properties: wave vector \mathbf{k} , complex electric vector \mathbf{E} and wavefront curvature \mathcal{Q} (Fig. 1). (ii). All properties of a ray after its interaction with a dioptric surface are calculated by the wavefront equation, the vectorial Snell law and the Fresnel formulas in wave vector components. (iii). In the region without singularity, the total field is the summation of the complex amplitudes of all the rays at that point, (iv). In the vicinity of singular points (caustics, critical angles, particle surface, ...), the singularity theory along with the uniform approximation will be applied. The physical optics (PO)[9, 27], the diffraction integration[21], etc. are examples of the special cases. The first three principles form VCRM, key progress on the interaction of a wave with a large non-spherical object, and the fourth one is based on the results of VCRM.

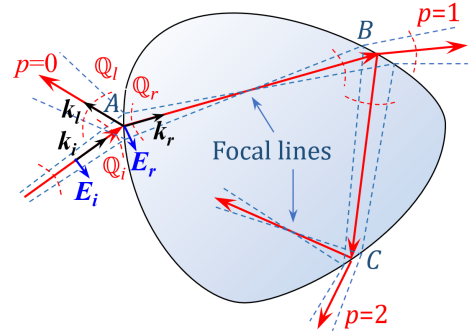


FIG. 1. Ray tracing in RTW.

Vectorial Complex Ray Model – The *wavefront equation* describes the relation between the wavefront curvatures of the incident wave and the refracted or re-

flected wave as function of the curvature of the diopter. It is at the heart of VCRM and we will derivate it for three dimension (3D) scattering.

Consider a ray incident on a curved surface Γ (blue in Fig. 2) at a point O . When an adjacent ray passing by the point A on the incident wavefront Σ (black in Fig. 2) reaches the diopter at H , the ray refracted at O arrives at E on the refracted wavefront Σ' (green in Fig. 2). We note B as the projection point of A on the tangent plane of Σ , C and G the projection points of H respectively on Γ and Σ' . The curvature of the surface Σ is described by its curvature matrix \mathbb{Q}_i in the base $(\hat{\mathbf{u}}_1, \hat{\mathbf{u}}_2)$. Similarly, the curvatures of Σ' and Γ are described respectively by their curvature matrices \mathbb{Q}_r and \mathbb{C} in the corresponding bases $(\hat{\mathbf{s}}_1, \hat{\mathbf{s}}_2)$ and $(\hat{\mathbf{v}}_1, \hat{\mathbf{v}}_2)$ (not presented in the figure for clarity). According to the differential geometry, in the vicinity of the tangent point, the distance between the point on the curved surface and the projected point on the tangent surface can be expressed as function of the curvature matrix. So, the infinitesimal distances $\delta_i = \overline{AB}$, $\delta_r = \overline{HG}$ and $\delta_c = \overline{HC}$ are given by

$$\delta_i = \frac{1}{2} \mathbf{t}_i \mathbb{Q}_i \mathbf{t}_i^T, \quad \delta_r = \frac{1}{2} \mathbf{t}_r \mathbb{Q}_r \mathbf{t}_r^T, \quad \delta_c = \frac{1}{2} \mathbf{t}_c \mathbb{C} \mathbf{t}_c^T$$

where $\mathbf{t}_i = \overrightarrow{OB}$, $\mathbf{t}_r = \overrightarrow{EG}$ and $\mathbf{t}_c = \overrightarrow{OC}$. The prime T stands for the transpose of a matrix. Note that the quantities δ and \mathbf{t} are all infinitely small, but the differential symbol d of $d\delta$ and $d\mathbf{t}$ is omitted here for clarity.

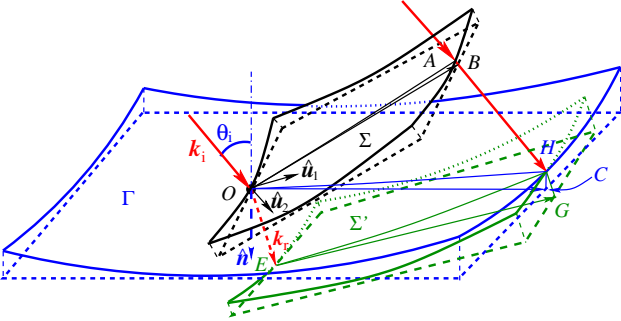


FIG. 2. Schema of the wavefronts and the diopter: an arbitrary wave incident on a curved surface.

The phase difference between the two wavefronts Σ and Σ' being constant, so $k_i \overline{AH} = k_r \overline{OE}$. On the other hand, from the geometry we have $\overline{AH} = \delta_i + \mathbf{t}_c \cdot \hat{\mathbf{k}}_i - \delta_c \hat{\mathbf{n}} \cdot \hat{\mathbf{k}}_i$ and $\overline{OE} = \delta_r + \mathbf{t}_c \cdot \hat{\mathbf{k}}_r - \delta_c \hat{\mathbf{n}} \cdot \hat{\mathbf{k}}_r$. These lead to

$$k_i(\delta_i + \mathbf{t}_c \cdot \hat{\mathbf{k}}_i - \delta_c \hat{\mathbf{n}} \cdot \hat{\mathbf{k}}_i) = k_r(\delta_r + \mathbf{t}_c \cdot \hat{\mathbf{k}}_r - \delta_c \hat{\mathbf{n}} \cdot \hat{\mathbf{k}}_r)$$

The terms $k_i \mathbf{t}_c \cdot \hat{\mathbf{k}}_i$ and $k_r \mathbf{t}_c \cdot \hat{\mathbf{k}}_r$ are independent of any curvatures, so we have $k_{i,\tau} = k_{r,\tau}$. This is also true for the reflected ray $k_{i,\tau} = k_{l,\tau}$. We establish thus the Snell law in vector form: the tangent components of the incident, reflected and refracted wave vectors are equal.

$$k_{i,\tau} = k_{l,\tau} = k_{r,\tau} \quad (1)$$

The rest of the equation gives rise to

$$k_i \mathbf{t}_i \mathbb{Q}_i \mathbf{t}_i^T - k_r \mathbf{t}_r \mathbb{Q}_r \mathbf{t}_r^T = \hat{\mathbf{n}} \cdot (\mathbf{k}_i - \mathbf{k}_r) \mathbf{t}_c \mathbb{C} \mathbf{t}_c^T \quad (2)$$

We express now \mathbf{t}_i and \mathbf{t}_r as function of \mathbf{t}_c by using the projection relations

$$\mathbf{t}_i = \mathbb{P}_i \mathbf{t}_c + \mathcal{O}(\mathbf{t}_i), \quad \mathbf{t}_r = \mathbb{P}_r \mathbf{t}_c + \mathcal{O}(\mathbf{t}_r) \quad (3)$$

where \mathbb{P}_i and \mathbb{P}_r are the projection matrices of the diopter base $(\hat{\mathbf{s}}_1^i, \hat{\mathbf{s}}_2^i)$ respectively on the incident and refracted wavefront bases $(\hat{\mathbf{u}}_1, \hat{\mathbf{u}}_2)$ and $(\hat{\mathbf{v}}_1, \hat{\mathbf{v}}_2)$

$$\mathbb{P}_i = \begin{pmatrix} \hat{\mathbf{s}}_1^i \cdot \hat{\mathbf{u}}_1 & \hat{\mathbf{s}}_1^i \cdot \hat{\mathbf{u}}_2 \\ \hat{\mathbf{s}}_2^i \cdot \hat{\mathbf{u}}_1 & \hat{\mathbf{s}}_2^i \cdot \hat{\mathbf{u}}_2 \end{pmatrix}, \quad \mathbb{P}_r = \begin{pmatrix} \hat{\mathbf{s}}_1^r \cdot \hat{\mathbf{v}}_1 & \hat{\mathbf{s}}_1^r \cdot \hat{\mathbf{v}}_2 \\ \hat{\mathbf{s}}_2^r \cdot \hat{\mathbf{v}}_1 & \hat{\mathbf{s}}_2^r \cdot \hat{\mathbf{v}}_2 \end{pmatrix} \quad (4)$$

Eq. (2) is then written as

$$\mathbf{t}_c (k_i \mathbb{P}_i \mathbb{Q}_i \mathbb{P}_i^T - k_r \mathbb{P}_r \mathbb{Q}_r \mathbb{P}_r^T) \mathbf{t}_c^T = \hat{\mathbf{n}} \cdot (\mathbf{k}_i - \mathbf{k}_r) \mathbf{t}_c \mathbb{C} \mathbf{t}_c^T \quad (5)$$

\mathbf{t}_c being arbitrary, we deduce finally the wavefront equation

$$k_r \mathbb{P}_r \mathbb{Q}_r \mathbb{P}_r^T = k_i \mathbb{P}_i \mathbb{Q}_i \mathbb{P}_i^T + \mathbb{C} \hat{\mathbf{n}} \cdot (\mathbf{k}_r - \mathbf{k}_i) \quad (6)$$

The wavefront equations given in [11] and [14] (sec. 4.2) correspond to the special case where one of the principal direction is in the incident plane. In the case of scattering in a symmetric plane, Eq. (6) is reduced to two scalar equations which are the same as those obtained by Hamilton optics in [22] (p 49) and [9] (p 186):

$$k_r \kappa_{r1} = k_i \kappa_{i1} + (k_{rn} - k_{in}) \kappa_{c1} \quad (7)$$

$$\frac{k_{rn}^2}{k_r} \kappa_{r2} = \frac{k_{in}^2}{k_i} \kappa_{i2} + (k_{rn} - k_{in}) \kappa_{c2} \quad (8)$$

where the indice 1 and 2 indicate respectively the principal curvatures in the directions perpendicular and parallel to the symmetric plane.

The two equations (1) and (6) tell all what we need for the vectorial complex ray tracing: the directions of the rays and their wavefront structure. With some simple considerations described below, we can calculate the complex amplitude of all rays at any point.

The amplitude of a ray, in the propagation of a wave and its interaction with an object, is affected by two factors: the Fresnel factor $\varepsilon_{X,p}$ and the divergence factor \mathcal{D} . The amplitude of the wave at a point M is then

$$A = A_0 |\varepsilon_{X,p}| \sqrt{\mathcal{D}} \quad (9)$$

where A_0 is the amplitude at the first incident point. $\varepsilon_{X,p}$ of p^{th} order emergent ray (Fig. 1) is given as

$$\varepsilon_{X,p} = \begin{cases} r_{X,0} & p = 0 \\ t_{X,0} t_{X,p} \prod_{q=1}^{p-1} r_{X,q} & p \geq 1 \end{cases} \quad (10)$$

$r_{X,q}$ and $t_{X,q}$ are respectively the Fresnel reflection and refraction coefficients of polarization X (\perp or \parallel) at the q^{th} interaction and given in RTW as function of the normal components k_{in} and k_{rn} , respectively, of the reflected and refracted wave vectors

$$r_{\perp} = \frac{k_{in} - k_{rn}}{k_{in} + k_{rn}}, \quad r_{\parallel} = \frac{m^2 k_{in} - k_{rn}}{m^2 k_{in} + k_{rn}} \quad (11)$$

$$t_{\perp} = \frac{2k_{in}}{k_{in} + k_{rn}}, \quad t_{\parallel} = \frac{2mk_{in}}{m^2 k_{in} + k_{rn}} \quad (12)$$

The divergence factor is

$$\mathcal{D} = \left| \frac{\kappa_{G2}}{\kappa'_{G1}} \cdot \frac{\kappa_{G3}}{\kappa'_{G2}} \cdots \frac{\kappa_{GM}}{\kappa_{Gq}} \right| \quad (13)$$

where κ_{Gq} and κ'_{Gq} are respectively the Gaussian curvatures of the wavefronts of the incident and refracted/reflected waves at q^{th} interaction point, and κ_{GM} the Gaussian curvature of the wavefront at the point M . The relation between the principal wavefront curvatures at two successive points are given by

$$\kappa_{\mu,q+1} = 1/(1/\kappa_{\mu,q} - d) \quad (14)$$

where $\mu = 1, 2$ and d is the distance between the two points.

The phase of a ray may change due to the reflection Φ_F , the optical path Φ_P and the focal lines Φ_f [6, 23]. Φ_F is determined by the argument of the Fresnel factor

$$\Phi_F = \arg(\varepsilon_{X,p}) \quad (15)$$

Φ_P is computed directly according to the optical path. Let \mathbf{r}_i and \mathbf{k}_i be respectively the position vector and the wave vector of the incident wave at the i^{th} interaction point, Φ_P of a ray after q interactions with the particle is given by

$$\Phi_P = -\mathbf{k}_1 \cdot \mathbf{r}_1 + \mathbf{k}'_q \cdot \mathbf{r}_q + \sum_{i=1}^{q-1} \mathbf{k}_{i+1} \cdot (\mathbf{r}_{i+1} - \mathbf{r}_i) \quad (16)$$

where \mathbf{k}'_q is the wave vector of the emergent ray.

Each time a wave passes a focal line (Fig. 1) the phase jumps a value of $\pi/2$ [19, 23]. This phenomenon corresponds to the sign changes of the wavefront curvatures, so the calculation of Φ_f in VCRM is just a matter to count the number N_f of sign changes of the wavefront curvatures, thus

$$\Phi_f = N_f \frac{\pi}{2} \quad (17)$$

If the incident wave is not a plane wave, its phase Φ_i at the first incident point should be counted. So the phase of a ray at the observation point M is

$$\Phi(M) = \Phi_i + \Phi_F + \Phi_P + \Phi_f \quad (18)$$

Eqs. (9)-(18) permit to calculate the amplitudes and the phases of all rays by ray tracing (Fig. 1). Finally, the properties of all the rays at any point are determined by Eqs. (1), (9) and (18).

Singularity correction – VCRM improves significantly the flexibility and the precision of classical ray model, but it still fails to predict correctly the field in the vicinity of the singularity points. However, it can calculate the complex electric field at any point rigorously in the sense of ray model and directly for a given object. The singularity theory[6] and the uniform approximation[5] can then be applied for the remedy. By a heuristic example, we have shown[27] that VCRM permits to reveal clearly the origin of the imprecision in the Airy theory and by replacing the polynomial function with directly calculated field, our method predicts very good results compared to the rigorous theory.

Thanks to the rapid development of computing technology, the polynomial or other approximate functions used in the singularity theory[4] can be replaced by the directly calculated field of VCRM. This should improve the precision and the flexibility in the singularity correction. This step needs a strategy special to RTW.

Strategy of RTW – In VCRM the forward ray tracing is used, i.e. the directions of the emergent rays are determined by the incident rays. To obtain the field at a given point or a given direction, a special strategy is to be employed.

Traditionally, a physical problem is considered solved if the relation between a physical quantity Y and its variables $\mathbf{x} = \{x_i\}(i = 1, 2, \dots)$ is established rigorously or approximately in the form $Y = \mathcal{F}(\mathbf{x}; \boldsymbol{\alpha})$, where $\boldsymbol{\alpha} = \{\alpha_j\}(j = 1, 2, \dots)$ are the problem related parameters and the operator \mathcal{F} can be in usual or special functions, a differential or integral operator, or their combination. The Mie theory and Airy theory are two typical examples. Otherwise, we establish an implicit relation between Y and \mathbf{x} in the form $\mathcal{F}(Y, \mathbf{x}; \boldsymbol{\alpha}) = 0$ then solve the equation numerically. This is largely used in the electromagnetic computation.

RTW uses neither of the two strategies. We express Y and \mathbf{x} through a set of intermediate variables $\mathbf{t} = \{t_i\}$: $Y = \mathcal{F}_1(\mathbf{t}; \boldsymbol{\alpha})$ and $\mathbf{x} = \mathcal{F}_2(\mathbf{t}; \boldsymbol{\alpha})$ and calculate Y and \mathbf{x} in a relevant range of \mathbf{t} , then establish the relationship between Y and \mathbf{x} with numerical technique. For instance to obtain the scattering field, we calculate the amplitudes and the phase $Y = (A, \Phi)$, and the directions of all the emergent rays $\mathbf{x} = (\theta, \phi)$ as function of the incident rays $\mathbf{t} = (\theta_i, \phi_i)$ and the particle properties $\boldsymbol{\alpha}$. The interpolation is applied to calculate the total complex amplitude of all rays in the interested region with[27] or without [13] wave effect correction.

Examples of applications – VCRM has been applied successfully to the simulation of the rainbow pattern of an oblate ellipsoid [12]. But two discernible discrepancies are observed when compared to the experimental results

(Fig. 6 in [12]). The first in the vicinity of the caustics is caused by the wave effect. We will show that the combination of VCRM with PO used in [27] for a spherical particle can be extended to a non-spherical particle. The second in the large scattering angles is due probably to experimental uncertainty. So we will compare the results of RTW with those of a rigorous numerical method.

TABLE I. Peak positions (in deg.) of supernumerary bows of a sphere (refractive index $m = 1.333$, $\lambda = 0.6328 \mu\text{m}$).

$a = 50 \mu\text{m}$				$a = 500 \mu\text{m}$			
K	Airy	RTW	Debye	K	Airy	RTW	Debye
0	139.50	139.47*	139.47	0	138.26	138.26*	138.26
1	142.98	142.88	142.87	1	139.01	139.00	139.00
2	145.41	147.24	147.23	21	145.13	144.98	149.99
4	149.37	149.01	148.99	41	149.14	148.81	148.81
6	152.72	152.14	152.12	61	152.53	151.97	151.97
8	155.73	154.91	154.88	81	155.55	154.76	154.76
10	158.51	157.43	157.39	101	158.34	157.29	157.29
12	161.10	159.77	159.72	121	160.95	159.64	159.64

* calculated by combination of VCRM and PO.

To ease the understanding, we begin with the classical problem – rainbow of a spherical drop. After the first satisfactory explanation of Descartes[10], Airy proposed a theory to calculate the scattering pattern of a rainbow[3]. Since almost two centuries, his theory has been studied by many researchers from different points of view[1, 10]. At the same time scientists have been wondering its precision from the beginning[8, 10] and tried to improve it[15, 16]. We have shown recently that by using the amplitude and the phase calculated with VCRM our method predict very precisely the rainbow patterns[27]. It is shown further in Tab. I that pure VCRM permits to predict very precisely all the supernumerary peaks except the main one ($K = 0$) which needs the combination of VCRM and PO. Tab. I reveals also the fact that, contrary to what believed commonly[23], the precision of Airy theory is almost independent of the particle size if observed at given angles.

To demonstrate the applicability of RTW to objects of any shape, we show the scattering patterns in the first and second rainbows of an oblate spheroid calculated by MLFMA and RTW in Fig. 3, top half for MLFMA and bottom half for VCRM. The computation for MLFMA[26] with an angle resolution of 0.1° has taken 997 GB memory (Intel Xeon Platinum 8276 CPU) and 40 hour CPU time with 160 threads. The computation time for VCRM on PC (Intel i9-13900ks, RAM 32 GB) is 9.4 min. for an angle resolution of 0.01° . The agreement of the two methods are very good including the fine structure except in the vicinity of the caustics. This could be remedied by PO with 2D diffraction integration that we are working on. Instead, a quantitative comparison of the scattering diagram on the symmetric plane $\psi = 0$ is given in Fig. 4. The result of RTW has been calcu-

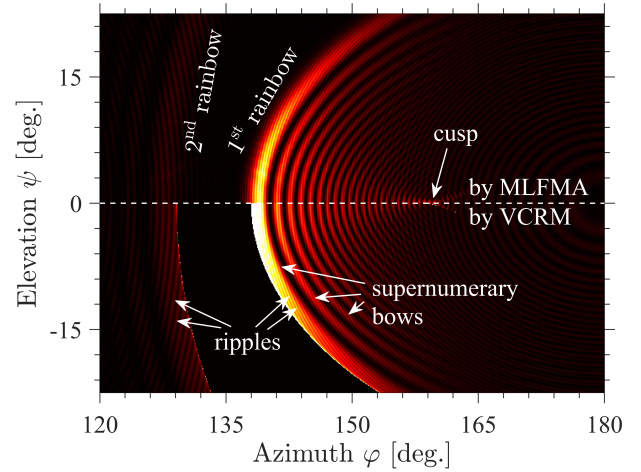


FIG. 3. Comparison of the scattering patterns calculated by VCRM and MLFMA for an oblate spheroid of semi-axes $a = b = 100 \mu\text{m}$, $c = 90 \mu\text{m}$ of water $m = 1.333$. The incident plane wave of wavelength $\lambda = 0.6328 \mu\text{m}$ is along x -axis.

lated by simple integration. It is clear that RTW is in good agreement with MLFMA, not only in the vicinity of the rainbow angles but also in the Alexander region. The discrepancy around 160° is due to 2D caustics which needs 2D integration.

Conclusions – The fundamentals and the strategy of the *Ray Theory of Waves* for scattering of large non-spherical objects with smooth surface are presented. The efficiency and the precision of RTW are demonstrated by comparison of the scattering patterns of an ellipsoidal drop calculated by RTW and MLFMA. The singularity correction for 3D scattering is to be developed[6, 21]. The applications of RTW in the domains concerning the interaction of waves with objects of irregular shape are also to be explored.

Acknowledgements This work was partially supported by the National Natural Science Foundation of China under Grants 62231003 and 62205262, the Agence Nationale de la Recherche (ANR-13-BS090008-01, AMO-COPS) of France and CRIANN (Normandy, France).

* Corresponding authors:

fang.ren@coria.fr,
xehan@mail.xidian.edu.cn,
yangminglin@bit.edu.cn

- [1] J. A. Adam. The mathematical physics of rainbows and glories. *Physics Reports*, 356:229–365, 2002.
- [2] J. A. Adam. *Rays, Waves, and Scattering*. Princeton University Press, 2017.
- [3] G. Airy. On the intensity of light in the neighbourhood of a caustic. *Trans. Cambridge Philos. Soc.*, 6(268):379–403, 1938.
- [4] M. Berry and C. Upstill. Catastrophe optics: Morpholo-

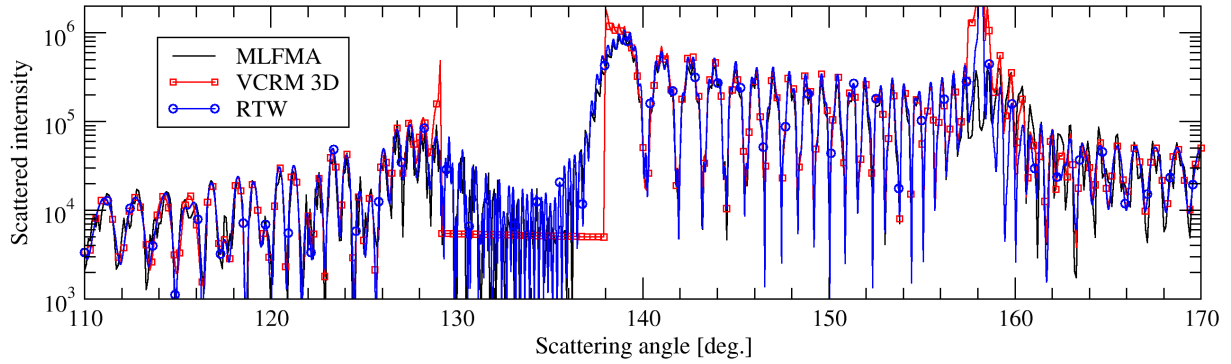


FIG. 4. Numerical comparison of the scattering diagrams in the plane $z = 0$ calculated by three methods MLFMA, VCRM and RTW with the same parameters as in Fig. 3.

- gies of caustics and their diffraction patterns. In *Prog. Opt.* Elsevier, 1980.
- [5] M. V. Berry. Uniform approximation: a new concept in wave theory. *Sci. Progress*, 57(225):43–64, 1969.
- [6] M. V. Berry. The singularities of light: intensity, phase, polarisation. *Light Sci Appl.*, 12(238):1–4, 2023.
- [7] L. Bi and P. Yang. Physical-geometric optics hybrid methods for computing the scattering and absorption properties of ice crystals and dust aerosols. In *Light Scattering Reviews*, pages 69–114. Springer-Praxis, 2013.
- [8] M. Boitel. Sur les arcs surnuméraires qui accompagnent l’arc-en-ciel. *Comptes rendus de l’Acad. Sci.*, CVI:1522–1524, 1888.
- [9] M. Born and E. Wolf. *Principles of optics*, 7th ed. Cambridge University Press, 1999.
- [10] C. B. Boyer. *The Rainbow, From Myth to Mathematics*. Princeton University Press, 1987.
- [11] G. A. Deschamps. Ray techniques in electromagnetics. *Proc. IEEE*, 60(9):1022–1035, 1972.
- [12] Q. Duan, F. R. A. Onofri, X. Han, and K. F. Ren. Generalized rainbow patterns of oblate drops simulated by a ray model in three dimensions. *Opt. Lett.*, 46(18):4585–4588, 2021.
- [13] Q. Duan, F. R. A. Onofri, X. Han, and K. F. Ren. Numerical implementation of three-dimensional vectorial complex ray model and application to rainbow scattering of spheroidal drops. *Optics Express*, 31(21):34980–35002, 2023.
- [14] G. L. James. *Geometrical theory of diffraction for electromagnetic waves*. Petter Peregrinus LTD., IEEE edition, 1980.
- [15] V. Khare and H. M. Nussenzveig. Theory of the rainbow. *Phys. Rev. Lett.*, 33:976–980, 1974.
- [16] G. P. Können and J. H. de Boer. Polarized rainbow. *Appl. Opt.*, 18(12):1961–1965, 1979.
- [17] P. L. Marston, editor. *Selected papers on geometrical aspects of scattering*. SPIE, United States, 1994. Title of Book: Selected papers on geometrical aspects of scattering. Editors of Book: P.L. Marston.
- [18] M. I. Mishchenko, J. W. Hovenier, and L. D. Travis. *Light Scattering by Nonspherical Particles: Theory, Measurements, and Applications*. Academic Press, San Diego, 2000.
- [19] K. F. Ren, F. Onofri, C. Rozé, and T. Girasole. Vectorial complex ray model and application to two-dimensional scattering of plane wave by a spheroidal particle. *Opt. Lett.*, 36(3):370–372, 2011.
- [20] X. Q. Sheng and W. Song. *Essentials of computational electromagnetics*. Wiley, Singapore, 2012.
- [21] J. J. Stamnes. *Wave in focal regions*. Adam Hilger, institute of physics publishing edition, 1986.
- [22] J. L. Synge. *Geometrical optics, an introduction to Hamilton’s method*. Cambridge University Press, 1937.
- [23] H. C. van de Hulst. *Light scattering by small particles*. John Wiley & Sons, New York, 1957.
- [24] Y. Wu, M. Yang, X. Sheng, and K. F. Ren. Computation of scattering matrix elements of large and complex shaped absorbing particles with multilevel fast multipole algorithm. *J. Quant. Spectrosc. Radiat. Transfer*, 156:88–96, 2015.
- [25] Y. M. Wu and W. C. Chew. The modern high frequency methods for solving electromagnetic scattering problems. *Progress EIM Res.*, 156:63–82, 2016.
- [26] M. L. Yang, B. Y. Wu, H. W. Gao, and X. Q. Sheng. A ternary parallelization approach of mlfma for solving electromagnetic scattering problems with over 10 billion unknowns. *IEEE Transactions on Antennas and Propagation*, 67(11):6965–6978, 2019.
- [27] C. Zhang, C. Rozé, and K. F. Ren. Airy theory revisited with the method combining vectorial complex ray model and physical optics. *Opt. Lett.*, 47(9):2149–2152, 2022.